

# The chemical evolution of galaxies within the IGIMF theory: the $[\alpha/\text{Fe}]$ ratios and downsizing.

S. Recchi<sup>1,2\*</sup>, F. Calura<sup>3\*\*</sup>, and P. Kroupa<sup>4\*\*\*</sup>

<sup>1</sup> Institute of Astronomy, Vienna University, Türkenschanzstrasse 17, A-1180, Vienna, Austria

<sup>2</sup> INAF - Osservatorio Astronomico di Trieste, Via G.B. Tiepolo 11, 34143 Trieste, Italy

<sup>3</sup> Astronomy Department, Trieste University, Via G.B. Tiepolo 11, 34143 Trieste, Italy

<sup>4</sup> Argelander Institute for Astronomy, Bonn University, Auf dem Hügel 71, 53121 Bonn, Germany

Received; accepted

## ABSTRACT

**Context.** The chemical evolution of galaxies is investigated within the framework of the star formation rate (SFR) dependent integrated galactic initial mass function (IGIMF).

**Aims.** We study how the global chemical evolution of a galaxy and in particular how  $[\alpha/\text{Fe}]$  abundance ratios are affected by the predicted steepening of the IGIMF with decreasing SFR.

**Methods.** We use analytical and semi-analytical calculations to evaluate the mass-weighted and luminosity-weighted  $[\alpha/\text{Fe}]$  ratios in early-type galaxies of different masses.

**Results.** The models with the variable IGIMF produce a  $[\alpha/\text{Fe}]$  vs. velocity dispersion relation which has the same slope as the observations of massive galaxies, irrespective of the model parameters, provided that the star formation duration inversely correlates with the mass of the galaxy (downsizing). These models also produce steeper  $[\alpha/\text{Fe}]$  vs.  $\sigma$  relations in low-mass early-type galaxies and this trend is consistent with the observations. Constant IMF models are able to reproduce the  $[\alpha/\text{Fe}]$  ratios in large elliptical galaxies as well, but they do not predict this change of slope for small galaxies. In order to obtain the best fit between our results and the observations, the downsizing effect (i.e. the shorter duration of the star formation in larger galaxies) must be milder than previously thought.

**Key words.** Stars: abundances – stars: luminosity function, mass function – supernovae: general – Galaxies: evolution – Galaxies: elliptical and lenticular, cD – Galaxies: star clusters

## 1. Introduction

It is nowadays widely accepted that most stars in galaxies form in star clusters (Tutukov 1978; Lada & Lada 2003). This has been observed in a number of different galaxies; from the Milky Way to the dwarf galaxies of the Local Group (Wyse et al. 2002; Massey 2003; Piskunov et al. 2004). Within each star cluster, the initial mass function (IMF) can be well approximated by the canonical two-part power-law form  $\xi(m) \propto m^{-\alpha}$  (e.g. Pflamm-Altenburg, Weidner & Kroupa 2007, hereafter PWK07). Massey & Hunter (1998) have shown that for stellar masses  $m >$  a few  $M_{\odot}$  a slope similar to the Salpeter (1955) index (i.e.  $\alpha = 2.35$ ) can approximate well the IMF in clusters and OB associations for a wide range of metallicities, whereas many studies have shown that the IMF flattens out below  $m \sim 1 M_{\odot}$  (Kroupa, Tout & Gilmore 1993; Chabrier 2001).

On the other hand, star clusters are also apparently distributed according to a single-slope power law,  $\xi_{\text{ecl}} \propto M_{\text{ecl}}^{-\beta}$ , where  $M_{\text{ecl}}$  is the stellar mass of the embedded star cluster. There is a general consensus that this slope  $\beta$  should be of the order of  $\sim 2$  (Zhang & Fall 1999; Lada & Lada 2003; Hunter et al. 2003), although a  $\beta$  as high as 2.4 can also be realistic (Weidner, Kroupa & Larsen 2004). According to this correlation, small em-

bedded clusters are more numerous in galaxies. They provide therefore most of the stars but not most of the massive ones, since they are preferentially formed in massive clusters (Weidner & Kroupa 2006). As a consequence of this mass distribution of embedded clusters, the integrated IMF in galaxies, the IGIMF, can be steeper than the stellar IMF within each single star cluster (Kroupa & Weidner 2003; Weidner & Kroupa 2005).

The Salpeter IMF slope has been used in a very wide range of modelling, providing good fits with observations concerning the cosmic star formation history (Calura, Matteucci & Menci 2004), the X-ray properties of elliptical galaxies (Pipino et al. 2005), the chemical evolution of dwarf galaxies (Larsen, Sommer-Larsen & Pagel 2001) and of the Milky Way (Pilyugin & Edmunds 1996, but see also Romano et al. 2005). Broadly speaking, a flatter than Salpeter IMF produces a larger fraction of massive stars. The large production of oxygen (and of  $\alpha$ -elements in general) leads to lower  $[\text{Z}/\text{O}]$  metallicity ratios. A steep IMF slope would instead be biased towards low- and intermediate-mass stars, underproducing oxygen and therefore resulting in larger  $[\text{N}/\text{O}]$  and  $[\text{C}/\text{O}]$  abundance ratios. On the other hand, iron will also be overproduced compared to  $\alpha$ -elements, since it comes mainly from Type Ia SNe which originate from C-O deflagration of binary systems of intermediate mass. Therefore, galaxies characterized by a steep IMF will tend to have  $[\alpha/\text{Fe}]$  ratios lower than models in which the IMF is flat.

The scenario of a variable integrated galactic initial mass function (IGIMF) has been applied in models of chemical evolu-

Send offprint requests to: S. Recchi

\* simone.recchi@univie.ac.at

\*\* fcalura@oats.inaf.it

\*\*\* pavel@astro.uni-bonn.de

tion (Köppen, Weidner & Kroupa 2007), producing an excellent agreement with the mass-metallicity relation found by Tremonti et al. (2004). However, these authors consider only the effect of the IGIMF on the global metallicity and the evolution of abundance ratios has not yet been explored in the literature. In a series of papers we plan to study the impact of the IGIMF on the abundance ratios in different classes of galaxies, using different methodologies. In this paper we study, by means of simple analytical and semi-analytical models, the evolution of  $[\alpha/\text{Fe}]$  ratios in galaxies, in particular in early-type ones. It is, in fact, now well established that the  $[\alpha/\text{Fe}]$  ratios in the cores of elliptical galaxies increase with galactic mass (Weiss, Peletier & Matteucci 1995; Kuntschner et al. 2001) and this poses serious problems to the current paradigm of hierarchical build-up of galaxies (see e.g. Thomas et al. 2005, hereafter THOM05; Nagashima et al. 2005; Pipino, Silk & Matteucci 2009; Calura & Menci, in preparation). In fact, in the classical hierarchical models the most massive ellipticals take a longer time to assemble and therefore form stars for a longer time than less massive galaxies, thus producing a trend of  $[\alpha/\text{Fe}]$  vs. mass which is opposite of what is observed (see Thomas, Maraston & Bender 2002; Matteucci 2007).

We will show in this paper that the trend of increasing  $[\alpha/\text{Fe}]$  vs. galaxy mass is naturally accounted for in models of elliptical galaxies in which the IGIMF is implemented. The second paper of this series will be devoted to the study of the chemical evolution of the Solar Neighborhood and of the local dwarf galaxies and in this case we will make use of detailed chemical evolution models. Another paper of this series will study the evolution of galaxies by means of chemodynamical models, in order to analyze how the IGIMF changes the feedback of the ongoing star formation in galaxies and how this affects the chemical evolution.

The plan of the present paper is as follows. In Sect. 2 we summarize the IGIMF theory and the formulations we adopt. In Sect. 3 we describe how we calculate the Type Ia and Type II SN rates in galaxies in which the SFR is given. Once we know the Type Ia and Type II SN rates, it is possible to calculate the  $[\alpha/\text{Fe}]$  ratios. This has been done in Sect. 4 for ellipticals and early-type galaxies in general. A discussion and the main conclusions are presented in Sect. 5.

## 2. The determination of the integrated galactic initial mass function

The determination of the IGIMF has been described previously (Kroupa & Weidner 2003; Weidner & Kroupa 2005; PWK07). The IGIMF theory is based on the assumption that all the stars in a galaxy form in star clusters. Surveys of star-formation in the local Milky Way disk have shown that 70 to 90 % of all stars appear to form in embedded clusters (Lada & Lada 2003; Evans et al. 2008). The remaining 10-30 % of the apparently distributed population may stem from a large number of short-lived small clusters that evolve rapidly by dissolving through energy equipartition and residual gas expulsion. It is therefore reasonable to assume that star formation occurs in embedded clusters with masses ranging from a few  $M_\odot$  upwards. The IGIMF, integrated over the whole population of embedded clusters forming in a galaxy, becomes

$$\xi_{\text{IGIMF}}(m; \text{SFR}(t)) = \int_{M_{\text{ecl,min}}}^{M_{\text{ecl,max}}(\text{SFR}(t))} \xi(m \leq m_{\text{max}}) \xi_{\text{ecl}}(M_{\text{ecl}}) dM_{\text{ecl}}, \quad (1)$$

where  $M_{\text{ecl,min}}$  and  $M_{\text{ecl,max}}(\text{SFR}(t))$  are the minimum and maximum possible masses of the embedded clusters in a population

of clusters and  $m_{\text{max}} = m_{\text{max}}(M_{\text{ecl}})$  (eqs. 3 and 4). For  $M_{\text{ecl,min}}$  we take  $5 M_\odot$  (the mass of a Taurus-Auriga aggregate, which is arguably the smallest star-forming "cluster" known), whereas the upper mass of the embedded cluster population depends on the SFR. The correlation between  $M_{\text{ecl,max}}$  and SFR has been determined observationally (Larsen & Richtler 2000; Weidner et al. 2004) and can be expressed with the correlation

$$\log M_{\text{ecl,max}} = \log k_{\text{ML}} + 0.75 \log \psi + 6.77, \quad (2)$$

where  $\psi$  is the SFR in  $M_\odot \text{ yr}^{-1}$  and  $k_{\text{ML}}$  is the mass-to-light ratio, typically 0.0114 for young stellar populations (Smith & Gallagher 2001). This empirical finding can be understood to result from the sampling of clusters from the embedded cluster mass function given the amount of gas mass being turned into stars per unit time (Weidner et al. 2004).

The stellar IMF (i.e. the IMF within each embedded cluster) has the canonical form  $\xi(m) = km^{-\alpha}$ , with  $\alpha = 1.3$  for  $0.08 M_\odot \leq m < 0.5 M_\odot$  and  $\alpha = 2.35$  (i.e. the Salpeter slope) for  $0.5 M_\odot \leq m < m_{\text{max}}$ , where  $m_{\text{max}}$  depends on the mass of the embedded cluster. In order to determine  $m_{\text{max}}$  and the proportionality constant  $k$  we have to solve the following two equations (Kroupa & Weidner 2003):

$$M_{\text{ecl}} = \int_{m_{\text{low}}}^{m_{\text{max}}} m \xi(m) dm, \quad (3)$$

$$\int_{m_{\text{max}}}^{m_{\text{max}*}} \xi(m) dm = 1, \quad (4)$$

where  $m_{\text{low}}$  is the smallest considered stellar mass ( $0.08 M_\odot$  in our case) and  $m_{\text{max}*}$  is the upper physical stellar mass and its value is assumed to be  $150 M_\odot$  (Weidner & Kroupa 2004). Eq. 4 indicates that, by definition of  $m_{\text{max}}$ , there is only one and exactly one star in the embedded cluster with mass  $M_{\text{ecl}}$  whose mass is larger than or equal to  $m_{\text{max}}$ .

The last ingredient we need is the distribution function of embedded clusters,  $\xi_{\text{ecl}}(M_{\text{ecl}})$ , which, as we have mentioned in the Introduction, we can assume proportional to  $M_{\text{ecl}}^{-\beta}$ . In this work we have assumed 3 possible values of  $\beta$ : 1.00 (model BETA100), 2.00 (model BETA200) and 2.35 (model BETA235). In Fig. 1 we have plotted the resulting IGIMFs for different values of SFR. In particular, we have tested 20 SFRs, ranging from  $10^{-4}$  to  $100 M_\odot \text{ yr}^{-1}$ , equally spaced in logarithm. To appreciate better the differences between various models, we have plotted in Fig. 2 IGIMFs for 3 different values of the SFR:  $\text{SFR} \approx 10^{-2} M_\odot \text{ yr}^{-1}$  (heavy lines),  $\text{SFR} \approx 1 M_\odot \text{ yr}^{-1}$  (middle lines),  $\text{SFR} \approx 10^2 M_\odot \text{ yr}^{-1}$  (light lines). We have considered all the possible values of  $\beta$ : model BETA100 (dashed lines), BETA200 (dotted lines), BETA235 (solid lines). For clarity, we have plotted the IGIMFs only for masses larger than  $\sim 2 M_\odot$ , since in the range of low mass stars the IGIMFs do not vary. As expected, the model with the steepest distribution of embedded clusters (model BETA235) produces also the steepest IGIMFs. This is due to the fact that model BETA235 is biased towards embedded clusters of low mass, therefore the probability of finding high mass stars in this cluster population is lower.

We can also notice from Fig. 2 that the differences between IGIMFs with  $\text{SFR} \approx 1 M_\odot \text{ yr}^{-1}$  (middle lines) and  $\text{SFR} \approx 10^2 M_\odot \text{ yr}^{-1}$  (light lines) are not very pronounced. This is due to the fact that for both these SFRs, the maximum possible mass of the embedded cluster is very high (see eq. 2), therefore in both cases the upper possible stellar mass of the whole galaxy is very close to the theoretical limit of  $150 M_\odot$ . This can be seen in Fig. 3

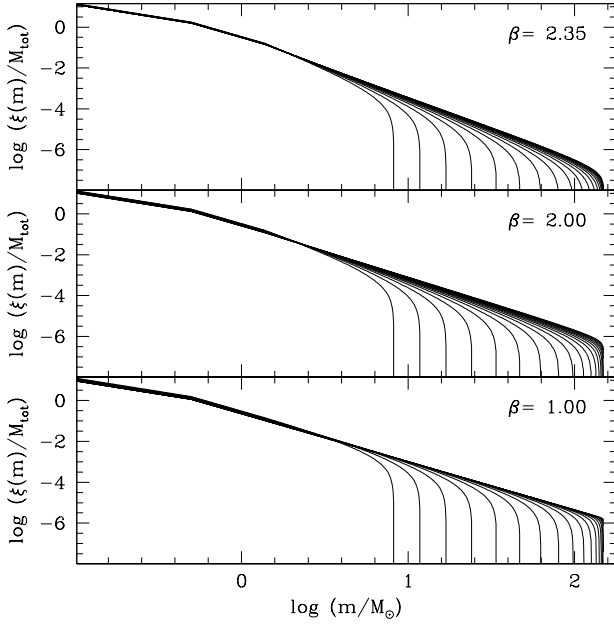


**Fig. 1.** IGIMFs for different distributions of embedded clusters (e.g. different values of  $\beta$ ). Upper panel: model BETA235; central panel: model BETA200; lower panel: model BETA100. For each panel we have considered 20 possible values of SFR, ranging from  $10^{-4} \text{ M}_{\odot} \text{ yr}^{-1}$  (lowermost curves) to  $100 \text{ M}_{\odot} \text{ yr}^{-1}$  (uppermost curves), equally spaced in logarithm.

(lower panel) in which we plot the variation of  $m_{\text{max}}$  as a function of SFR as deduced from eqs. 4 and 3. This correlation is valid for all the possible values of  $\beta$  because it is determined by  $\xi(m)$  and not by  $\xi_{\text{ecl}}(M_{\text{ecl}})$ . As we can see from Figs. 1 and 2, the IGIMFs are characterized by a nearly uniform decline, which follows approximately a power law, and a sharp cutoff when  $m$  gets close to  $m_{\text{max}}$ . In Fig. 3 (upper panel) we plot therefore also the slope that better approximates the IGIMF in the range 3 - 16  $\text{M}_{\odot}$ . This is the range of masses where most of the progenitors of SNeII and SNeIa originate (see Sect. 3). Of course, the steeper the distribution of embedded clusters is, the steeper the corresponding IGIMFs are. Fig. 3 shows also what we have noticed before, namely that the various IGIMFs saturate for  $\text{SFR} > 1 \text{ M}_{\odot} \text{ yr}^{-1}$ . Finally, in Fig. 3 (middle panel)  $k_{\alpha}$  is shown as a function of the SFR for the various models.  $k_{\alpha}$  is the number of stars per unit mass in one stellar generation (see e.g. Greggio 2005) and its value is given by

$$k_{\alpha} = \frac{\int_{m_{\text{low}}}^{m_{\text{max}}} \xi_{\text{IGIMF}}(m) dm}{\int_{m_{\text{low}}}^{m_{\text{max}}} m \xi_{\text{IGIMF}}(m) dm}. \quad (5)$$

This parameter is useful to calculate the SNII rates (see Sect. 3).

### 3. The determination of Type Ia and Type II SN rates

#### 3.1. Type II SN rates

Stars in the range  $m_{\text{up}} < m < m_{\text{max}}$  (where  $m_{\text{up}}$  is the mass limit for the formation of a degenerate C–O core) are generally supposed to end their lives as *core-collapse* SNe. These SNe divide into SNeII, SNeIb and SNeIc according to their spectra. For our purposes, this distinction is not useful and we will suppose that

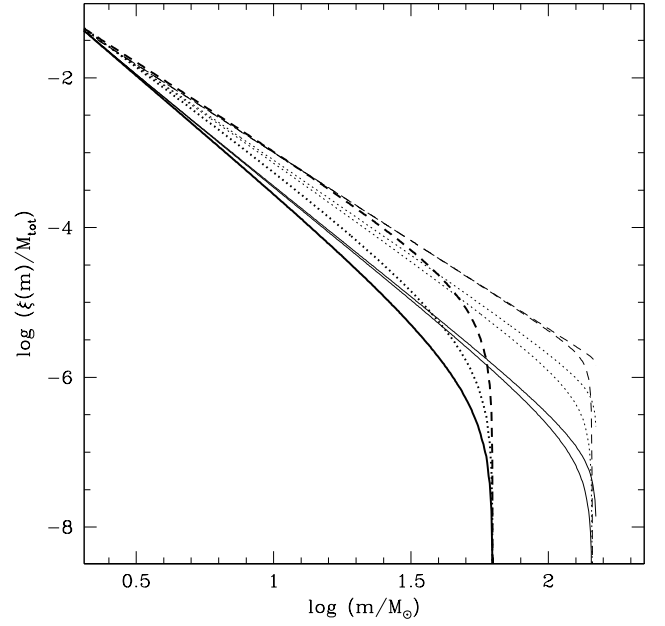


**Fig. 2.** IGIMFs for different SFRs:  $\approx 10^{-2} \text{ M}_{\odot} \text{ yr}^{-1}$  (heavy lines);  $\approx 1 \text{ M}_{\odot} \text{ yr}^{-1}$  (middle lines);  $\approx 10^2 \text{ M}_{\odot} \text{ yr}^{-1}$  (light lines). We have considered all the possible values of  $\beta$ : model BETA100 (dashed lines), BETA200 (dotted lines), BETA235 (solid lines).

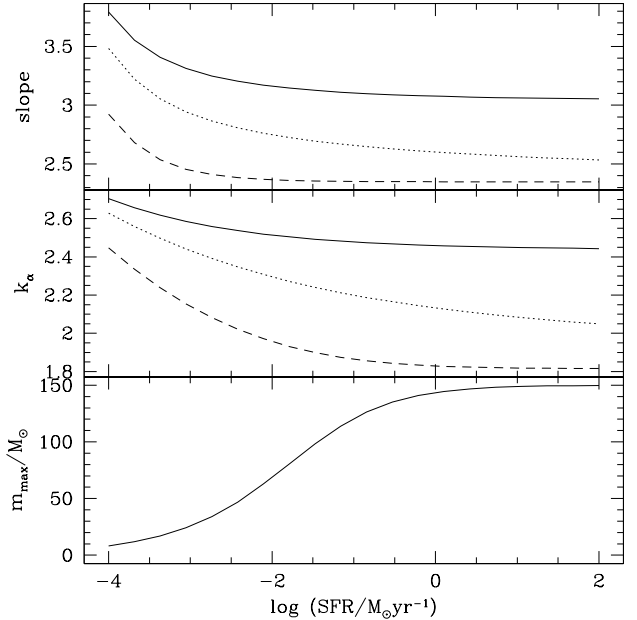


**Fig. 3.** Lower panel:  $m_{\text{max}}$  (in  $\text{M}_{\odot}$ ) as a function of SFR (in  $\text{M}_{\odot} \text{ yr}^{-1}$ ). Middle panel:  $k_{\alpha}$  (number of stars per unit mass in one stellar generation). Upper panel: IGIMF slopes in the range 3 - 16  $\text{M}_{\odot}$ . Notations as in Fig. 2.

all the core-collapse supernovae are indeed SNeII. These SNe produce the bulk of  $\alpha$ -elements and some iron (one third approximately). The standard value of  $m_{\text{up}}$  is 8  $\text{M}_{\odot}$  but stellar models with overshooting predict lower values (e.g. Marigo 2001). However, stars more massive than  $m_{\text{up}}$  can still develop a de-

generate O–Ne core and end their lives as electron-capture SNe (Siess 2007). We will assume for simplicity that all the stars with masses larger than  $8 M_{\odot}$  end their lives as SNeII, therefore the SNII rate is simply given by the rate at which massive stars die, namely:

$$R_{\text{SNII}}(t) = \int_8^{m_{\text{max}}} \psi(t - \tau_m) \xi_{\text{IGIMF}}[m, \psi(t - \tau_m)] dm, \quad (6)$$

where  $\psi$  is the SFR and  $\tau_m$  is the lifetime of a star of mass  $m$ . The lifetime function is adapted from the work of Padovani & Matteucci (1993),

$$\tau_m = \begin{cases} 1.2m^{-1.85} + 0.003 \text{ Gyr} & \text{if } m \geq 6.6 M_{\odot} \\ 10^{f(m)} \text{ Gyr} & \text{if } m < 6.6 M_{\odot}, \end{cases} \quad (7)$$

where

$$f(m) = \frac{[0.334 - \sqrt{1.79 - 0.2232 \times (7.764 - \log(m))}]}{0.1116}. \quad (8)$$

In eq. 6 the IGIMF is calculated by considering the SFR at the time  $t - \tau_m$ , therefore it depends both on time and on mass.

It is instructive to analyze models in which SFR is constant during the whole evolution of the galaxy. In this way, eq. 6 simplifies into

$$R_{\text{SNII}} = \psi \int_8^{m_{\text{max}}} \xi_{\text{IGIMF}}(m, \psi) dm = \psi k_{\alpha} n_{>8}, \quad (9)$$

where, as we have seen in Sect. 2,  $k_{\alpha}$  is the number of stars per unit mass in one stellar generation (therefore  $\psi k_{\alpha}$  is the number of stars formed per unit time) and  $n_{>8}$  is the number fraction of stars with masses larger than  $8 M_{\odot}$ . In Fig. 4 (lower panel) we plot  $R_{\text{SNII}}$  (in  $\text{cen}^{-1}$ ) as a function of SFR for the 3 adopted values of  $\beta$ . It is worth pointing out that, even if SFR is constant,  $R_{\text{SNII}}$  starts increasing only after the star with mass  $m_{\text{max}}$  ends its life and reaches a constant value only after the lifetime of a  $8 M_{\odot}$  star. This lifetime ( $\sim 28$  Myr with the adopted lifetime function) is however negligible compared to the Hubble time, therefore it is reasonable to consider  $R_{\text{SNII}}$  constant with time. For SFRs larger than  $\sim 10^{-2} M_{\odot} \text{ yr}^{-1}$   $R_{\text{SNII}}$  increases almost monotonically with SFR, whereas it drops dramatically for  $\text{SFR} < 10^{-2} M_{\odot} \text{ yr}^{-1}$ . This is mostly due to the drop of  $n_{>8}$  at low SFRs (Fig. 4, upper panel) which in turn depends on the fact that the upper mass  $m_{\text{max}}$  for these values of SFR starts reducing significantly and it gets very close to  $8 M_{\odot}$  for a SFR of  $10^{-4} M_{\odot} \text{ yr}^{-1}$  (Fig. 3), therefore only a very narrow interval of stellar masses gives rise to SNII explosions. From Fig. 3 we can see instead that the variation of  $k_{\alpha}$  with SFR is not very significant, therefore  $k_{\alpha}$  affects only mildly the Type II SN rates.

It is nowadays getting popular to consider SN rates normalized to the stellar mass of the considered galaxy. The usually chosen unit of measure is the SNum ( $1 \text{ SNum} = 1 \text{ SN } \text{cen}^{-1} 10^{-10} M_{*}^{-1}$ , where  $M_{*}$  is the current stellar mass of the galaxy). In this case, models in which the SFR is constant cannot attain a constant Type II SN rate in SNum since the stellar mass of the galaxy increases with time. We therefore calculated  $R_{\text{SNII}}$  in SNum as a function of time for the various models. The stellar mass of the galaxy at each time  $t$  is given by  $\int_0^t \psi \cdot f_{<m(t)} dt$ , where  $f_{<m(t)}$  is the mass fraction of stars, born until the time  $t$  that have not yet died.

Fig. 5 shows the evolution with time of the Type II SN rate for different models and different SFRs, assuming a constant

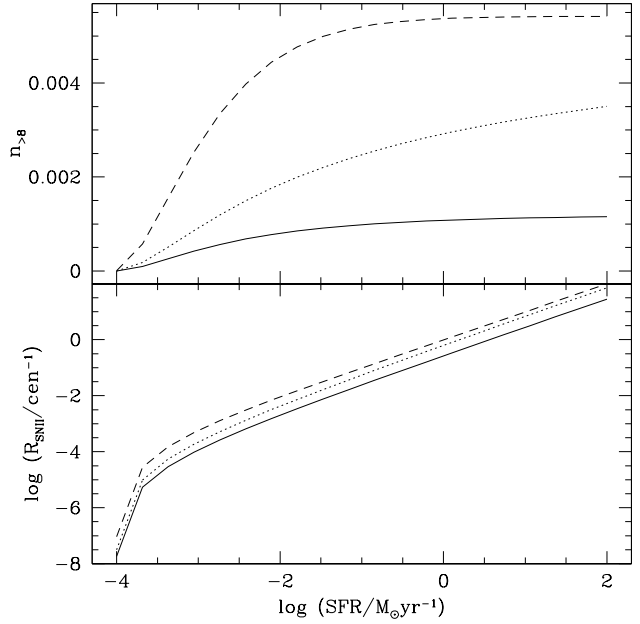


**Fig. 4.** Lower panel:  $R_{\text{SNII}}$  (in  $\text{cen}^{-1}$ ) as a function of SFR (in  $M_{\odot} \text{ yr}^{-1}$ ). Upper panel:  $n_{>8}$  (number fraction of stars more massive than  $8 M_{\odot}$ ) as a function of SFR. Notation as in Fig. 2.

SFR for 14 Gyr. These results are compared with the average SNeII rates (in SNum), observationally derived by Mannucci et al. (2005) in S0a/b galaxies (solid boxes), Sbc/d galaxies (dotted boxes) and irregular ones (dashed boxes). We can notice that, for the models BETA100 and BETA200 only the mildest SFRs can reproduce the final SNII rates in S0a/b galaxies, whereas model BETA235 can fit the final SNII rate of S0a/b galaxies for a wide range of SFRs. On the other hand, all the models predict final SNII rates significantly below the observations of irregular galaxies and the final values for model BETA235 fail also to fit the observed rates in Sbc/d galaxies. It is important to note, however, that the stellar mass in galaxies is usually calculated assuming some (constant) IMF. Under the assumption that the IMF changes with the SFR, the determinations of the stellar masses must be revisited. PWK07 showed that the IGIMF effect (i.e. the suppression of the number of massive stars with respect of low-mass stars) can be very significant in dwarf galaxies, whereas in large galaxies it tends to be very small. Moreover, a constant SFR for 14 Gyr is not a reasonable description of the star formation history of irregular (and Sbc/d) galaxies which often experience an increase of the SFR in the last Gyrs of their evolution (see e.g. Calura & Matteucci 2006). For this reason, the calculated SNII rates of late type galaxies tend to fit the observations at smaller ages.

### 3.2. Type Ia SN rates

In order to calculate the SNIa rates, we assume the so-called Single Degenerate Scenario of SNIa formation. It is commonly assumed that a SNIa explodes when a C–O white dwarf in a binary system reaches the Chandrasekhar mass after mass accretion from a companion star. According to the Single Degenerate channel of SNIa explosion, the accretion of matter occurs via mass transfer from a non-degenerate companion (a red giant or a main sequence star) filling its Roche lobe (Whelan & Iben 1973).

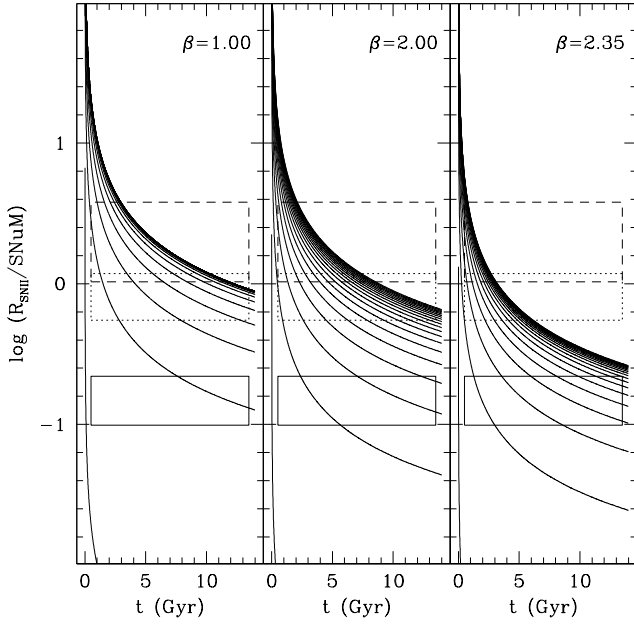


**Fig. 5.**  $R_{\text{SNI}}$  (in SNeM) as a function of time (in Gyr) for models with constant SFR and different values of  $\beta$ : model BETA100 (left panel), BETA200 (central panel), BETA235 (right panel). In each panel, the lowermost curve has  $\text{SFR} = 10^{-4} \text{ M}_{\odot} \text{ yr}^{-1}$ , the uppermost has  $\text{SFR} = 10^2 \text{ M}_{\odot} \text{ yr}^{-1}$  and the other SFRs are equally spaced in logarithm. Observations of the core-collapse SN rates in S0a/b galaxies (solid boxes), in Sbc/d galaxies (dotted boxes) and in irregular ones (short-dashed boxes) are also shown. Data are taken from Mannucci et al. (2005)

In this way, the SNIa rate depends on the number distribution of C-O white dwarfs, but also on the mass ratio between primary and secondary stars in a binary system. The SNIa rate in the framework of the Single Degenerate Scenario has been analytically calculated by a number of authors assuming a universal IMF (see Valiante 2009 and references therein). Here we follow the formulation of Greggio & Renzini (1983) and Matteucci & Recchi (2001) but we modify it to take into account that, in the framework of the IGIMF, the IMF changes according to the SFR. The SNIa rate in this case turns out to be:

$$R_{\text{Ia}}(t) = A \int_{m_{\text{B,inf}}}^{m_{\text{B,sup}}} \int_{\mu_{\text{min}}}^{0.5} f(\mu) \psi(t - \tau_{m_2}) \xi_{\text{IGIMF}}[m_{\text{B}}, \psi(t - \tau_{m_2})] d\mu dm_{\text{B}}, \quad (10)$$

where  $A$  is a normalization constant (assumed to be 0.09 in the following). Although theoretical arguments demonstrate that  $A$  should be small (e.g. Maoz 2008) its value is usually calibrated with the Milky Way. Unfortunately, our analytical approach does not allow us to simulate the Milky Way within the IGIMF theory, therefore we take 0.09 as a reference value and postpone a more careful discussion about it to the follow-up numerical paper (but see also Sec. 4 for a study of the variation of  $A$  for early-type galaxies).  $m_{\text{B}}$  is the total mass of the binary system,  $m_2$  is the mass of the secondary star,  $\mu = m_2/m_{\text{B}}$  and  $f(\mu)$  is the distribution function of mass ratios (see below). It is commonly assumed that the maximum stellar mass able to produce a degenerate C-O white dwarf is a  $8 \text{ M}_{\odot}$  star, therefore the maximum possible binary mass is  $16 \text{ M}_{\odot}$ . The minimum possible binary mass is assumed to be  $3 \text{ M}_{\odot}$  in order to ensure that the smallest possible white dwarf can accrete enough mass from the secondary star

to reach the Chandrasekhar mass. With these assumptions, the limits of integration in eq. (10) are:

$$m_{\text{B,inf}} = \max[2m_2(t), 3\text{M}_{\odot}] \quad (11)$$

$$m_{\text{B,sup}} = 8\text{M}_{\odot} + m_2(t), \quad (12)$$

$$\mu_{\text{min}} = \max\left[\frac{m_2(t)}{m_{\text{B}}}, \frac{m_{\text{B}} - 8\text{M}_{\odot}}{m_{\text{B}}}\right]. \quad (13)$$

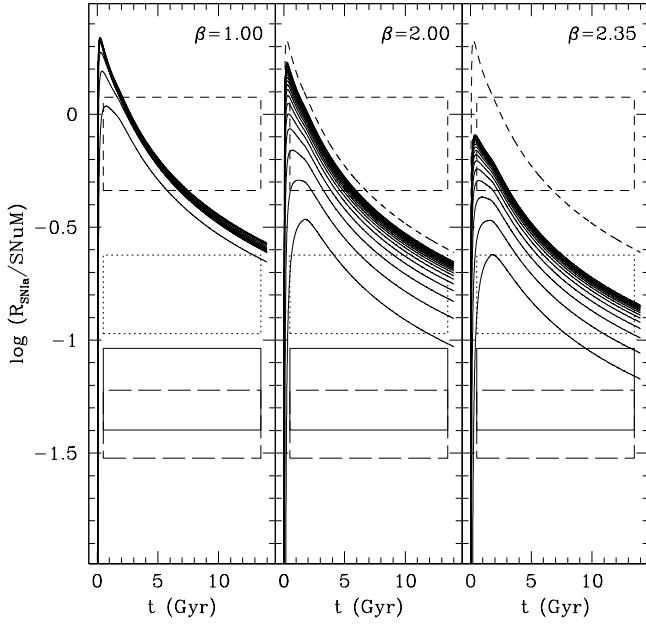
The distribution function of mass ratios is generally described as a power law ( $f(\mu) \propto \mu^{\gamma}$ ), but the value of  $\gamma$  is still much debated in the literature (Duquennoy & Mayor 1991; Shatsky & Tokovinin 2002; Kouwenhoven et al. 2005) and therefore we will take it as a free parameter.<sup>1</sup>

Fig. 6 shows the evolution with time of the Type Ia SN rate for different models and different SFRs, analogously to Fig. 5 for SNeII rates. Also shown (dashed lines) for comparison are SNIa rates obtained for a model with fixed (i.e. not SFR-dependent) IMF. We assume the canonical stellar IMF (i.e. the IMF within each embedded cluster) which, as mentioned in Sect. 2, has the form  $\xi(m) = km^{-\alpha}$ , with  $\alpha = 1.3$  for  $0.08 \text{ M}_{\odot} < m < 0.5 \text{ M}_{\odot}$  and  $\alpha = 2.35$  above  $0.5 \text{ M}_{\odot}$ . As we can see, at large SFRs model BETA100 produces rates almost indistinguishable from the ones obtained with the fixed canonical IMF (see also Kroupa & Weidner 2003). In this figure  $\gamma$  is assumed to be 2 (Tutukov & Yungelson 1980). This large value of  $\gamma$  favors the occurrence of SNeIa in binary systems with similar masses. Such a steep mass ratio distribution that favors equal-mass binaries may result from dynamical evolution of stellar populations in long-lived star clusters (Shara & Hurley 2002). We can notice again that only model BETA235 at very low SFRs seems able to reproduce the SNIa rates in S0a/b and E/S0 galaxies. However, we point out that the comparison with the observed SNIa rates in elliptical galaxies is meaningless because they have stopped forming stars several Gyr ago, therefore they have evolved passively since then. For them we cannot therefore assume a constant SFR for 14 Gyr (see Sect. 4). On the other hand, model BETA235 produces SNIa rates that only match the observed rates in dwarf irregular galaxies at their peak. Therefore, assuming  $\gamma = 2$ , the best value for  $\beta$  seems to be 2 (but see the comment in Sect. 3.1 about the possible inconsistency of the published determination of stellar masses, at least for irregular galaxies). To show the dependence of the results on  $\gamma$  we show in Fig. 7 the SNIa rates obtained assuming  $\gamma = 0.3$ . This flatter distribution function implies that a larger fraction of binary systems with small mass ratios end up as SNeIa. We can notice from this figure that the observed SNIa rates in spiral galaxies are reproduced by a larger range of SFRs, whereas the disagreement with the observed rates in irregular galaxies worsens.

#### 4. A test of the IGIMF: $[\alpha/\text{Fe}]$ ratios in early-type galaxies

The study of the average stellar  $[\alpha/\text{Fe}]$  ratio in galaxies represents an important constraint for our models, since this quantity depends both on the adopted galactic star formation history and on the stellar IMF (Matteucci 2001). In local ellipticals, the observed correlation between the central velocity dispersion  $\sigma$ , which reflects the total stellar mass, and the stellar  $[\alpha/\text{Fe}]$  is interpreted as due to the shorter star formation timescales in the most

<sup>1</sup> Note that usually observative papers adopt mass ratios  $q = m_2/m_1$  instead of  $\mu$  (Abt & Levy 1976). The mass ratio distribution function  $f(q)$  can be obtained from  $f(\mu)$  by means of a simple change of variable.



**Fig. 6.**  $R_{\text{SNIa}}$  (in SNU) as a function of time (in Gyr) for models with constant SFR. Notations and symbols as in Fig. 5, with the addition of the observed SNIa rate in E/S0 galaxies (long-dashed boxes) and the SNIa rates predicted assuming a constant IMF (dashed lines). Data are taken from Mannucci et al. (2005).

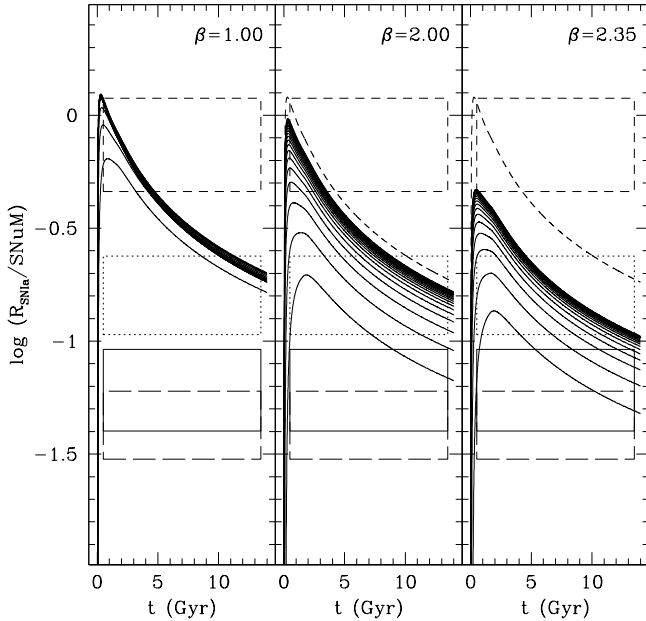


**Fig. 7.** As in Fig. 6 but for  $\gamma = 0.3$ .

massive galaxies (Pipino & Matteucci 2004; THOM05) which in turn implies also that the most massive galaxies experience the most intense episodes of star formation. For this reason, the average stellar  $[\alpha/\text{Fe}]$  vs  $\sigma$  relation represents a valuable test for the IGIMF, since the IGIMF is a function of the galactic star formation rate. The issue of a variable IMF among elliptical galaxies to explain the  $[\alpha/\text{Fe}]$  vs.  $\sigma$  relation has already been explored with

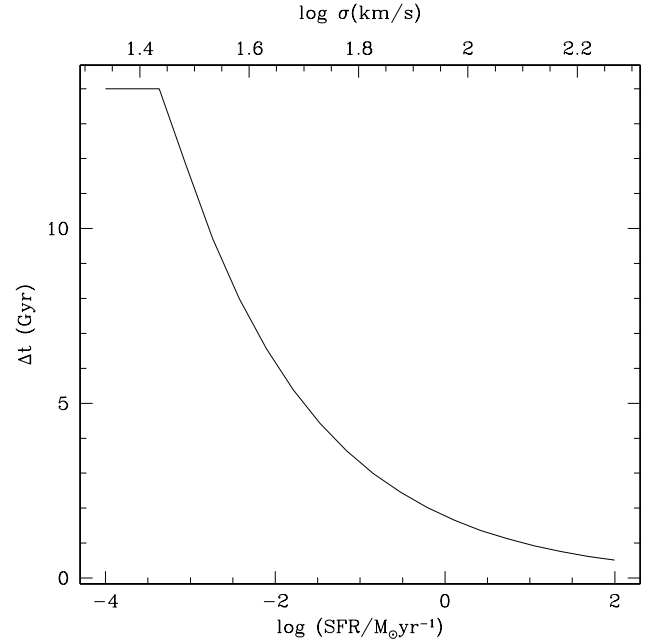


**Fig. 8.** Duration  $\Delta t$  of the star formation (assumed constant) as a function of SFR (lower scale) and  $\sigma$  (upper scale) assuming the  $\Delta t$ -luminous mass relation of THOM05 (see text).

success by Matteucci (1994) but assuming ad hoc variations of the IMF slope. In this section we test, using well-established and observationally constrained star formation histories of early-type galaxies of various masses, if the physically motivated IGIMF can equally well reproduce this correlation.

To simplify the calculations, the SFR is assumed to be constant over a period of time  $\Delta t$ . We have numerically tested that this crude approximation about the star formation history does not affect significantly the results. The value of  $\Delta t$  as a function of galaxy luminous mass is adopted from the work of THOM05, who, on the basis of the observational relation between  $[\alpha/\text{Fe}]$  and  $\sigma$ , showed the existence of a *downsizing* pattern for elliptical galaxies, according to which the smaller ellipticals form over longer timescales (see also Matteucci 1994; Cowie et al. 1996; Kodama et al. 2004). Since the present-day stellar mass is given in this case by  $\psi \cdot \int_0^{\Delta t} f_{\text{low}}(t) dt$  (where  $f_{\text{low}}(t)$  is the fraction of long-living stars, namely the stars, born at the time  $t$ , that live until the present day), it is possible to derive a relation between the SFR and the duration of the star formation activity  $\Delta t$ , which we show in Fig. 8. This relation saturates at 14 Gyr since this is assumed to be the age of the Universe. A similar relation can be recovered from the work of Pipino & Matteucci (2004) assuming that the star formation occurs only until the onset of the galactic wind, however the two SFR- $\Delta t$  relations do not significantly differ.

For each galaxy (characterized by a specific SFR over a period  $\Delta t$ ) we calculate the average yield from SNeII of a chemical element  $i$ ,

$$\overline{y_i^{\text{II}}} = \frac{\int_8^{m_{\text{max}}} y_i(m) \xi_{\text{IGIMF}}(m, \psi) dm}{\int_8^{m_{\text{max}}} \xi_{\text{IGIMF}}(m, \psi) dm}, \quad (14)$$

where  $y_i(m)$  is the yield of chemical element  $i$  produced by a single star of mass  $m$ . The nucleosynthetic prescriptions are taken from Woosley & Weaver (1995). We have however halved the

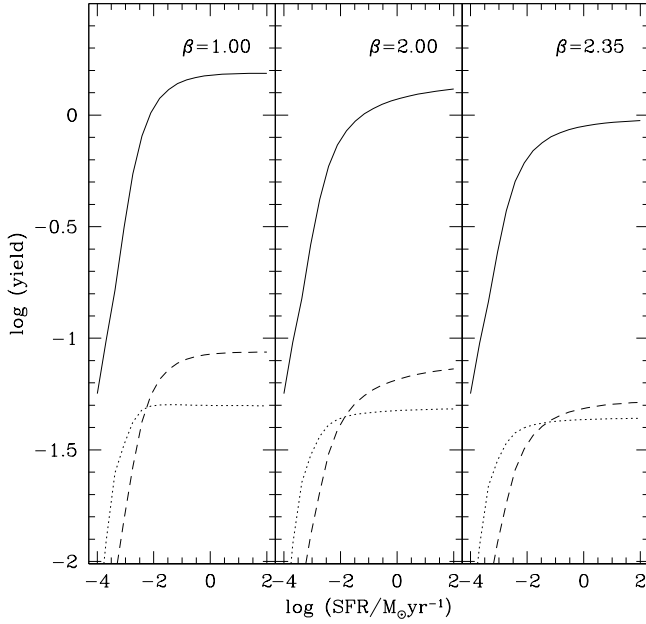


**Fig. 9.** IGIMF- averaged SNII yields of oxygen (solid lines), iron (dotted lines) and magnesium (dashed lines) as a function of SFR (in  $M_{\odot} \text{ yr}^{-1}$ ) for different values of  $\beta$ : model BETA100 (left panel), BETA200 (central panel), BETA235 (right panel).

iron yields, in accordance with Timmes, Woosley & Weaver (1995) and Chiappini, Matteucci & Gratton (1997), because it is known that only in this way it is possible to reproduce the  $[\alpha/\text{Fe}]$  in Galactic stars. Unfortunately, Woosley & Weaver (1995) calculated yields only for stellar masses up to  $40 M_{\odot}$ . We assume that the yields of stars more massive than  $40 M_{\odot}$  are equal to the  $40 M_{\odot}$  star yields. Given the very limited amount of stars in the range  $40 M_{\odot} < m < m_{\text{max}}$  the results are not sensitive to this assumption. In Fig. 9 we show the IGIMF-averaged SNII yields of oxygen (solid lines), iron (dotted lines) and magnesium (dashed lines) as a function of the SFR for different values of  $\beta$ . For what concerns SNIa, we assume the yields reported by Gibson, Loewenstein & Mushotzky (1997), based on the work of Thielemann, Nomoto & Hashimoto (1993).

Once we know the SNIa yields and the IGIMF-averaged SNII yields for each galaxy, we can calculate the mass fraction  $\frac{\alpha}{\text{Fe}}(t)$  (where  $\alpha$  is O or Mg) produced until the time  $t$  by using the formula:

$$\frac{\alpha}{\text{Fe}}(t) = \frac{\int_0^t (R_{\text{Ia}}(t)y_{\alpha}^{\text{Ia}} + R_{\text{SNII}}\overline{y}_{\alpha}^{\text{II}})dt}{\int_0^t (R_{\text{Ia}}(t)y_{\text{Fe}}^{\text{Ia}} + R_{\text{SNII}}\overline{y}_{\text{Fe}}^{\text{II}})dt}, \quad (15)$$

where  $R_{\text{Ia}}$  and  $R_{\text{SNII}}$  are the SNIa and SNII rates, given by eqs. 10 and 9, respectively, and  $y_{\alpha}^{\text{Ia}}$  are the SNIa yields.

At this point, we can compute the theoretical average stellar abundances by means of:

$$[\alpha/\text{Fe}] = \log_{10} \frac{\psi \cdot \int_0^{\Delta t} \frac{\alpha}{\text{Fe}}(t) \cdot f_{\text{low}}(t)dt}{M_{\text{tot}}} - \log_{10} \frac{\alpha_{\odot}}{\text{Fe}_{\odot}}. \quad (16)$$

where  $M_{\text{tot}}$  is the total present-day stellar mass and  $\alpha_{\odot}$  and  $\text{Fe}_{\odot}$  are the solar abundances of  $\alpha$ -elements and Fe, respectively, taken from Anders & Grevesse (1989). This means that our theoretical abundance ratios represent values mass-averaged over

the stars which survive until the present time (see also Thomas, Greggio & Bender 1999).

The observable in elliptical galaxies is the velocity dispersion instead of the mass, so in order to properly compare our results with observations we need to assume a correlation between the stellar mass and the velocity dispersion of galaxies (Faber-Jackson relation). We assume:

$$\sigma = 0.86 M_{\text{tot}}^{0.22}, \quad (17)$$

(Burststein et al. 1997), where  $\sigma$  is the velocity dispersion in km/s. The resulting relation between  $\sigma$  and  $\Delta t$  can be seen from Fig. 8 where we have indicated in the upper scale the  $\sigma$  corresponding to each SFR.

In Fig. 10 we show our results for  $\gamma = 0.3$  comparing our models with observations taken from THOM05 and references therein (filled squares). We can first notice that, as expected, the model BETA100 (heavy dashed lines), giving rise to flatter IGIMFs (see Fig. 1), produces larger  $[\alpha/\text{Fe}]$  ratios. In fact, flatter IGIMFs result in a larger fraction of massive stars and, therefore, to a larger production of  $\alpha$ -elements. We can also appreciate that the models reproduce quite well the  $[\alpha/\text{Fe}]$  (both  $[\text{O}/\text{Fe}]$  and  $[\text{Mg}/\text{Fe}]$ ) ratios in elliptical galaxies, at least for the models BETA200 and BETA235. To appreciate the effect of the IGIMF approach, we plot also (long-dashed line) a model with the fixed canonical IMF which, as mentioned in Sect. 2 and reminded in Sect. 3.2, has the form  $\xi(m) = km^{-\alpha}$ , with  $\alpha = 1.3$  for  $0.08 M_{\odot} < m < 0.5 M_{\odot}$  and  $\alpha = 2.35$  above  $0.5 M_{\odot}$ . The curves obtained with the IGIMF tend to flatten out at large  $\sigma$ , whereas the curve obtained with the constant IMF shows a constant slope. This demonstrates once more that the adoption of the IGIMF is particularly remarkable in the low-mass (and low- $\sigma$ ) galaxies. The curve with a constant IMF approaches asymptotically the model BETA100 since this model at large SFRs produces the flattest IMFs (see Fig. 1). Besides a small shift of a few tenths of dex (which can be fixed increasing the parameter  $A$  in Eq. 10), the curve with a constant IMF reproduces well the trend of  $[\alpha/\text{Fe}]$  vs.  $\sigma$  of the THOM05 sample, demonstrating that the downsizing (or inverse-wind) models (Matteucci 1994; Pipino & Matteucci 2004) are also perfectly capable of explaining this trend in large elliptical galaxies. However, evidence is mounting that  $[\alpha/\text{Fe}]$  ratios in early-type dwarf galaxies are solar or sub-solar. For instance, van Zee, Barton & Skillman (2004) showed that  $[\alpha/\text{Fe}]$  ratios (derived from Lick indices) of a sample of Virgo dwarf irregular galaxies range between -0.3 and solar. Also in the cluster Abell 496 the smallest galaxies show  $[\text{Mg}/\text{Fe}]$  to be solar or sub-solar (Chilingarian et al. 2008). To show that we have also plotted in Fig. 10 (open triangles) the data of a sample of low-mass early-type galaxies by Sansom & Norneast (2008). These data confirm that the  $[\alpha/\text{Fe}]$  vs.  $\sigma$  relation is probably steeper in the low-mass regime and that our IGIMF results can naturally predict this behavior. However, in order to properly test our results in the low-mass regime more data are needed.

It is worth pointing out that in this figure (and in the following ones) we have considered only model galaxies for which the SFR is smaller than  $100 M_{\odot} \text{ yr}^{-1}$ . This is the reason why the data points reach larger  $\sigma$  than the results of our model. In extreme starbursts the IMF might become top-heavy as evident by the mass-to-light ratios in ultra-compact dwarf galaxies which are ultra-massive “star clusters” that form when the SFR is very high (Dabringhausen, Kroupa & Baumgardt 2009) and this will need to be incorporated in the IGIMF calculations (work in preparation).

In general, in local early-type galaxies the stellar abundances are measured by means of various absorption-line Lick indices,

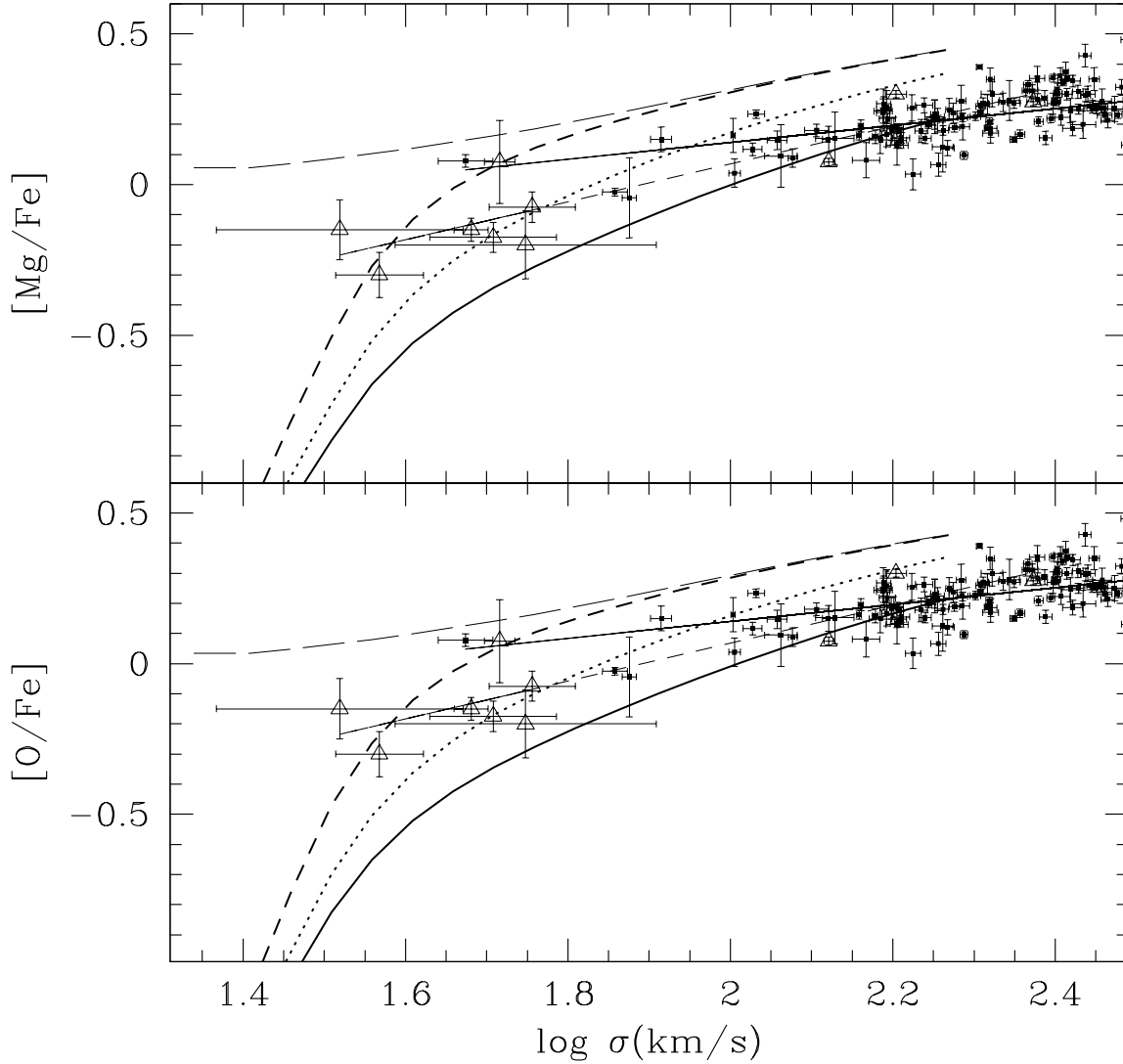


**Fig. 10.** Mass-weighted  $[\text{Mg}/\text{Fe}]$  (upper panel) and  $[\text{O}/\text{Fe}]$  (lower panel) vs.  $\sigma$  for models with a constant SFR over a period of time  $\Delta t$  which depends on the stellar mass of the galaxy (see text) assuming  $\gamma = 0.3$ . Heavy solid line: model BETA235; heavy dotted line: model BETA200; heavy short-dashed line: model BETA100; long-dashed line: model with a constant (i.e. not SFR-dependent) canonical IMF. The filled squares are the observational values and relative error-bars as reported by THOM05 and references therein and the light solid line is the least-square fit of this data. The open triangles are  $[\alpha/\text{Fe}]$  ratios reported by Sansom & Northeast (2008) and the light short-dashed line is the corresponding least-square fit.

such as  $\text{Mg } b$  and  $\langle Fe \rangle = 0.5(\text{Fe}52720 + \text{Fe}5335)$  (THOM05). To properly compare predictions to observational abundance data obtained for local ellipticals, in general one should derive the luminosity-weighted average abundances. The real abundances averaged by mass are larger than the luminosity-averaged ones, owing to the fact that, at constant age, metal-poor stars are brighter (Greggio 1997). To calculate the luminosities we have made use of the Starburst99 package (Leitherer et al. 1999; Vázquez & Leitherer 2005), producing  $L(t)$  for each value of SFR and  $\beta$ . The results are shown in Fig. 11 for the first 100 Myr (the luminosities remain almost constant after 100 Myr).

As expected, since model BETA100 is characterized by the flat-test IGIMFs, it produces also the largest luminosities. We have then calculated luminosity-weighted mass ratios by using the formula:

$$[\alpha/\text{Fe}] = \log_{10} \frac{\int_0^{\Delta t} \frac{\alpha}{\text{Fe}}(t) L(t) dt}{\int_0^{\Delta t} L(t) dt} - \log_{10} \frac{\alpha_{\odot}}{\text{Fe}_{\odot}}. \quad (18)$$

The results are shown in Fig. 12. As we can see, the results differ very little (by a few hundredths of dex at most) compared to the mass-averaged abundance ratios. We have checked these results also using the spectro-photometric code of Jimenez et



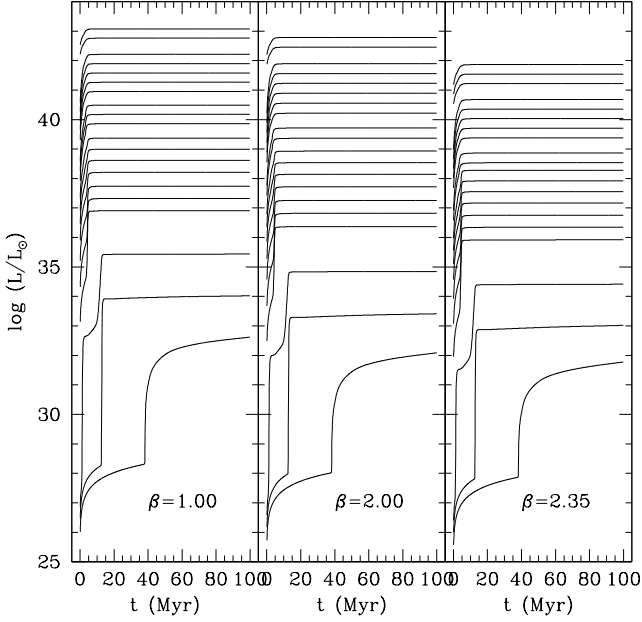


**Fig. 11.** Stellar luminosities (in  $L_{\odot}$ ) as a function of time (in Myr) for models with constant SFR and different values of  $\beta$ : model BETA100 (left panel), BETA200 (central panel), BETA235 (right panel). In each panel, the lowermost curve has  $\text{SFR} = 10^{-4} M_{\odot} \text{ yr}^{-1}$ , the uppermost has  $\text{SFR} = 10^2 M_{\odot} \text{ yr}^{-1}$  and the other SFRs are equally spaced in logarithm. These luminosities have been obtained with the Starburst99 package (Leitherer et al. 1999; Vázquez & Leitherer 2005)

al. (1998) (see also Calura & Matteucci 2003) but the results do not differ appreciably compared with the ones obtained with the Starburst99 package. Indeed, it has been already shown in the literature (but for constant IMFs) that the discrepancy for the  $[\text{Mg}/\text{Fe}]$  ratio computed by averaging by mass and by luminosity is very small, with typical values of 0.01 dex (Matteucci, Ponzzone & Gibson 1998; Thomas et al. 1999). We have confirmed this finding also in the case of the IGIMF.

To check how much our results depend on the assumption of a variable  $\Delta t$  with stellar mass, we plot in Fig. 13 the  $[\alpha/\text{Fe}]$  obtained assuming a constant value of  $\Delta t = 1$  Gyr. The agreement with the observations is still quite good; in particular the models maintain an increasing trend of  $[\alpha/\text{Fe}]$  with  $\sigma$ . However, the curves tend to flatten out too much at larger  $\sigma$ , at variance with the trend shown by the observations. This is due to the fact that, as pointed out in Sect. 2, the various IGIMFs for rates of star formation larger than  $1 M_{\odot} \text{ yr}^{-1}$  do not show very large differences. Therefore, the assumption of a star formation duration inversely proportional to the stellar mass of the galaxy (or in other words the downsizing) is a key ingredient to understand the chemical properties of large elliptical galaxies.

To appreciate the dependence on the distribution function of mass ratios in binary stars (the parameter  $\gamma$  introduced in Sect. 3.2) we plot in Figs. 14 and 15 the results of models with  $\gamma = 2.0$  and  $\gamma = -0.3$ , respectively. The curves obtained with  $\gamma = 2.0$  tend to be slightly steeper than the ones shown in Fig. 10 (and slightly steeper than the observations) but the agreement remains still good, in particular for the models BETA100 and BETA200. If we assume  $\gamma = -0.3$  an excellent match with the observations is instead provided by the model BETA235. Models BETA100

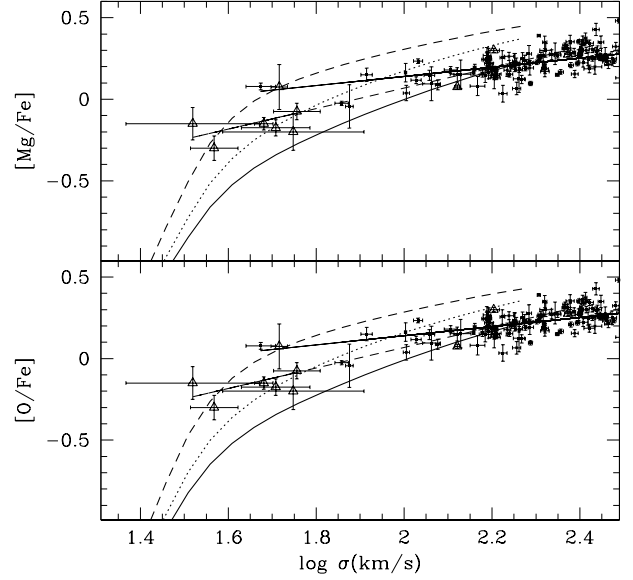


**Fig. 12.** As in Fig. 10 but with luminosity-weighted  $[\alpha/\text{Fe}]$  ratios, calculated by means of eq. 18.

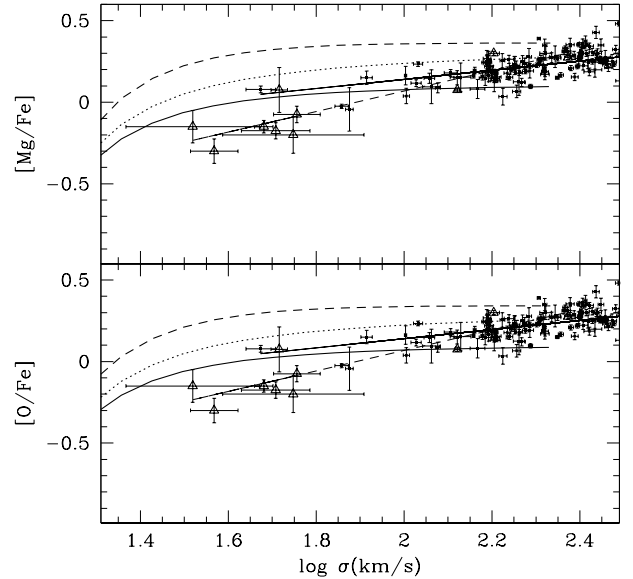


**Fig. 13.** As in Fig. 10 but with  $\Delta t = 1$  Gyr for each stellar mass.

and BETA200 show the same slope of the observational data but shifted by a few tenths of dex. A slight increase of the parameter  $A$  in eq. 10 would make these models perfectly compatible with the observations.

It is particularly remarkable that the trend of  $[\alpha/\text{Fe}]$  ratios vs.  $\sigma$  (namely an increase of  $[\alpha/\text{Fe}]$  with  $\sigma$ ) is naturally reproduced using the IGIMF approach, without any further assumption or fine-tuning of parameters. This is for instance at variance with what hierarchical clustering models of structure formation would tend to produce, since in this case larger elliptical galaxies

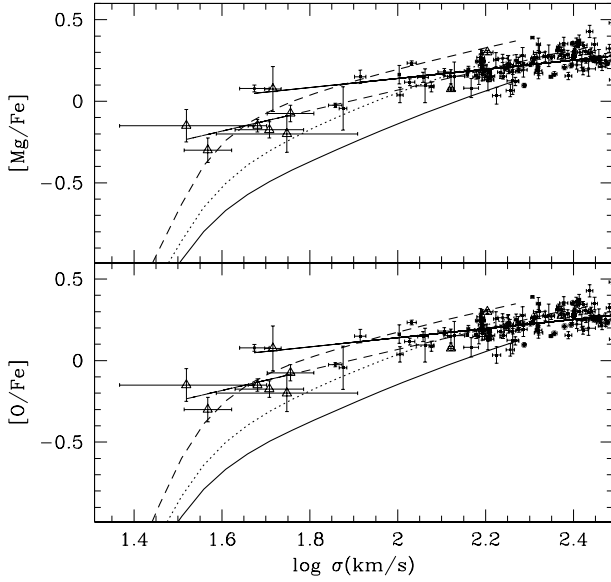


**Fig. 14.** As in Fig. 10 but with  $\gamma = 2.0$ .

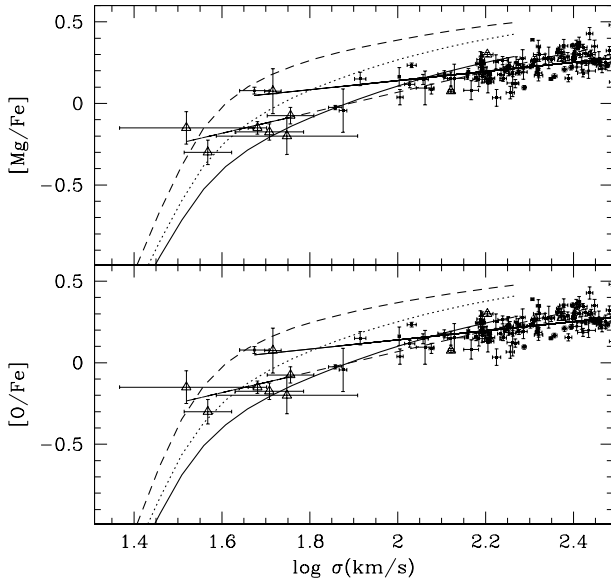


**Fig. 15.** As in Fig. 10 but with  $\gamma = -0.3$ .

are formed later, out of building blocks in which the  $[\alpha/\text{Fe}]$  ratio has already dropped (e.g. Thomas et al. 2002). It is worth mentioning that De Lucia et al. (2006), by means of a semi-analytical model adopting the concordance  $\Lambda$  CDM cosmology, suggested that more massive ellipticals should have shorter star formation timescales, but lower assembly (by dry mergers) redshift than less luminous systems. This is one of the first works based on the hierarchical paradigm for galaxy formation producing downsizing in the star formation histories of early-type galaxies through the inclusion of AGN feedback (see also Bower et al. 2006; Cattaneo et al. 2006), although they did not compute the  $[\alpha/\text{Fe}]$ –

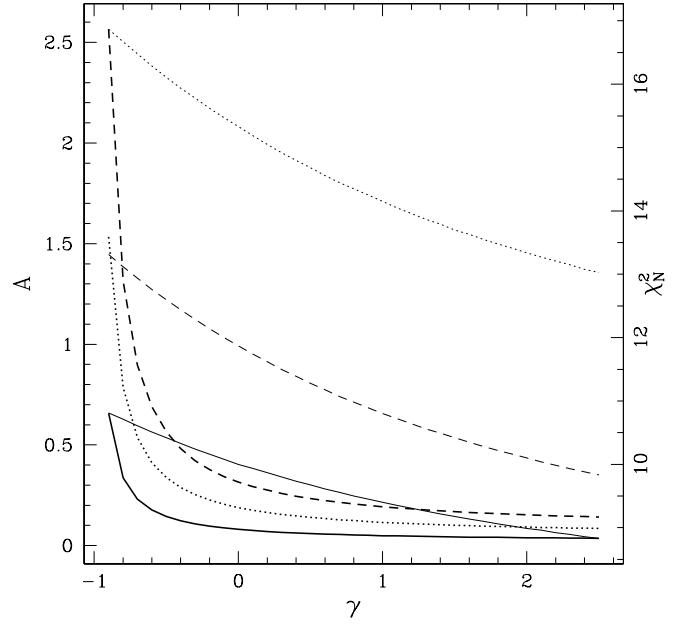


**Fig. 16.** Normalization constant  $A$  to adopt in order to obtain the best fit with the observational data as a function of  $\gamma$  for model BETA100 (heavy dashed line), BETA200 (heavy dotted line) and BETA235 (heavy solid line). The light lines represent, for each value of  $\beta$ , the normalized chi square of the represented model (scale on the right axis).

$\sigma$  relation for ellipticals. However, the lower assembly redshift for the most massive system is still in contrast to what is concluded by Cimatti, Daddi & Renzini (2006), who show that the downsizing trend should be extended also to the mass assembly, in the sense that the most massive ellipticals should have assembled before the less massive ones. Very recently, Pipino et al. (2008) showed that even in semi-analytical models able to account for the downsizing, the  $[\alpha/\text{Fe}]$  vs.  $\sigma$  relation is not reproduced.

Although the agreement between our results and the observations is good, none of the models presented so far fits perfectly the data at low and high  $\sigma$  simultaneously. In order to work out an overall best model, for each value of  $\gamma$  and  $\beta$  we have checked, by means of a minimization of the normalized chi square, which normalization constant  $A$  fits better the data. The results are shown in Fig. 16. As we can see, model BETA235 seems to be preferable and the best agreement between data and models is obtained for the model BETA235 with  $\gamma = 2.5$  and  $A = 0.036$ . In general, the best fits are obtained with large values of  $\gamma$ , although that requires low values of  $A$ . A large value of  $\gamma$ , favoring equal-mass binary systems, is consistent with the results of Shara & Hurley (2002), although observational surveys cited in Sect. 3.2 seem to indicate lower values of  $\gamma$ .

We should however not forget that the  $\Delta t$ –luminous mass relation we have used in this work has been obtained by THOM05 assuming a constant IMF. We have therefore checked, starting from our best model, namely a model with  $\beta = 2.35$ ,  $\gamma = 2.5$  and  $A = 0.036$ , how this relation should change in order to best fit the data. It turns out that, within the IGIMF theory, the best  $\Delta t$ –luminous mass relation is given by:

$$\log \Delta t = 2.38 - 0.24 \log M_{\text{tot}}, \quad (19)$$

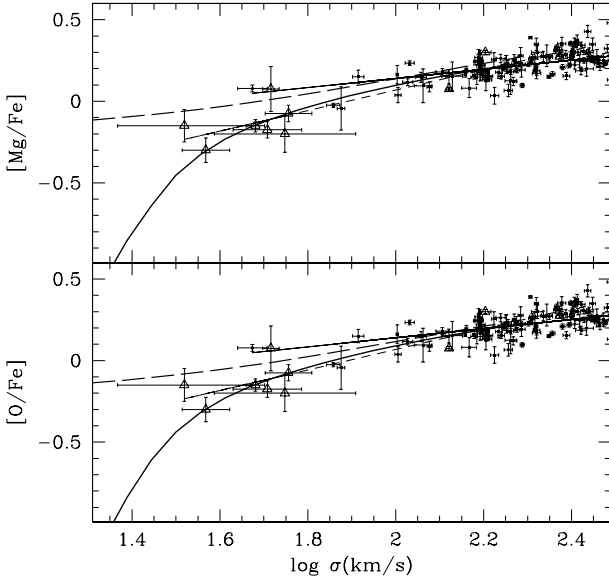


**Fig. 17.** Mass-weighted  $[\text{Mg}/\text{Fe}]$  (upper panel) and  $[\text{O}/\text{Fe}]$  (lower panel) vs.  $\sigma$  for our best IGIMF model (namely model BETA235 with  $\gamma = 2.5$  and  $A = 0.036$ ) with a  $\Delta t$ –luminous mass relation described by eq. 19 (heavy solid lines). Also shown (heavy long-dashed lines) a model with fixed, canonical IMF,  $\gamma = 2.5$  and  $A = 0.13$ . Notations and symbols as in Fig. 10

where  $\Delta t$  is in Myr and  $M_{\text{tot}}$  in  $M_{\odot}$ , and this relation produces the results shown in Fig. 17. We have also plotted in this figure a model with canonical stellar IMF (heavy long-dashed line) in which we have increased the value of  $A$  up to 0.13 in order to better reproduce the data. We can notice again that the canonical IMF can perfectly fit the  $[\alpha/\text{Fe}]$  ratios in large ellipticals but it shows a constant slope and therefore it cannot equally well reproduce the  $[\alpha/\text{Fe}]$  ratios in dwarf galaxies, at variance with the IGIMF model. The comparison between relation 19 and eq. 5 of THOM05 is displayed in Fig. 18. We can notice here that the *downsizing effect* (namely the shorter duration of the star formation in larger galaxies) is milder, in the sense that the  $\Delta t$  for large galaxies is (slightly) larger than the timescale calculated by THOM05, whereas at low  $\sigma$  the star formation durations are significantly lower than the ones predicted by THOM05.

## 5. Discussion and conclusions

In this paper we have studied, by means of analytical and semi-analytical calculations, the evolution of  $[\alpha/\text{Fe}]$  ratios in early-type galaxies and in particular their dependence on the luminous mass (or equivalently on the velocity dispersion  $\sigma$ ). We have applied the so-called integrated galactic initial mass function (IGIMF; Kroupa & Weidner 2003; Weidner & Kroupa 2005) theory, namely we have assumed that the IMF depends on the star formation rate (SFR) of the galaxy, in the sense that the larger the SFR is, the flatter is the resulting slope of the IGIMF. This kind of behavior would naturally tend to form more massive stars (and therefore more SNeII) in large galaxies, which are characterized by more intense star formation episodes. Therefore, it is expected that, since  $\alpha$ -elements are mostly formed by SNeII, the most massive galaxies are also the

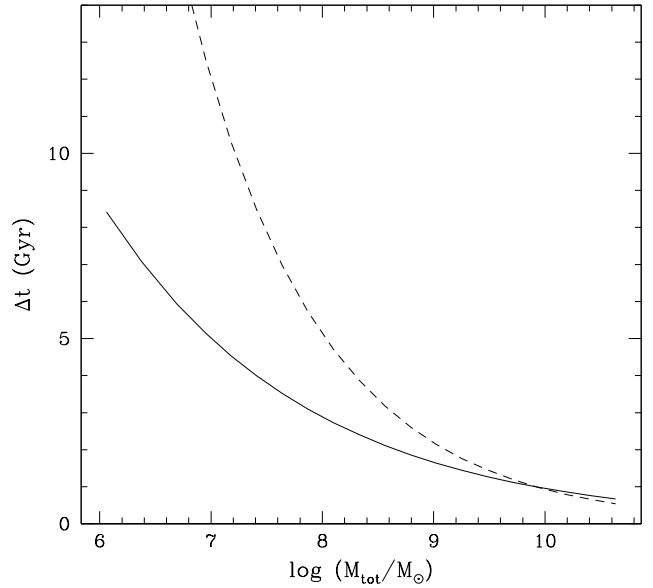


**Fig. 18.**  $\Delta t$ –luminous mass relation obtained with eq. 19 (solid line) and derived by THOM05 (their eq. 5; dashed line).

ones which attain the largest  $[\alpha/\text{Fe}]$  ratios, in agreement with the observations. One of the main aims of this paper was to quantitatively check whether the chemical evolution of galaxies within the IGIMF theory is able to accurately fit the observed  $[\alpha/\text{Fe}]$  vs.  $\sigma$  relation.

We have analytically calculated the SNeII and SNeIa rates with the IGIMF assuming 3 possible slopes of the distribution function of embedded clusters,  $\xi_{\text{ecl}} \propto M_{\text{ecl}}^{-\beta}$ , where  $M_{\text{ecl}}$  is the stellar mass of the embedded star cluster; in particular we have considered  $\beta = 1.00$  (model BETA100);  $\beta = 2.00$  (model BETA200);  $\beta = 2.35$  (model BETA235). We have seen that, if we consider constant SFRs over the whole Hubble time, the final SNeIa and SNeII rates agree quite well with the observations of spiral galaxies (in particular the S0a/b ones). The agreement with the observed rates in irregular galaxies is not good, but a constant SFR over the whole Hubble time is not likely in irregular galaxies, which probably have experienced an increase of the SFR in the last Gyrs of their evolution.

To calculate the  $[\alpha/\text{Fe}]$  ratios with the IGIMF we assumed that early-type galaxies form stars at a constant rate over a period of time  $\Delta t$  which depends on the total luminous mass of the considered galaxy. This hypothesis is based on the work of THOM05 who, on the basis of observational grounds, showed the existence of a downsizing pattern for elliptical galaxies, i.e. that the most massive galaxies are the ones with the shortest  $\Delta t$ . We have then calculated the production of  $\alpha$ -elements and Fe by SNeII (in particular we have calculated IGIMF-averaged SNeII yields) and by SNeIa and we have calculated mass-weighted and luminosity-weighted  $[\alpha/\text{Fe}]$  ratios for each model galaxy, characterized by different SFRs and  $\beta$ .

The resulting mass-averaged  $[\alpha/\text{Fe}]$  vs.  $\sigma$  relations show the same slope as the observations in massive galaxies as reported by THOM05, irrespective of the value of  $\beta$  and of the distribution function of mass ratios in binaries  $f(\mu) \propto \mu^{\gamma}$  (which affects the SNeIa rates), although models with  $\beta = 2.35$  and large values of  $\gamma$  seem to be preferable. Some models show a shift (of

a few tenths of dex) compared with the observations but this can be fixed increasing (or decreasing) the fraction,  $A$ , of binary systems giving rise to SNeIa, which is an almost unconstrained parameter. It is however remarkable that all the models we have calculated show the same trend of the observations because if, as commonly argued, large elliptical galaxies form out of mergers of smaller sub-structures (hierarchical clustering), it would be natural to expect that they are the ones with the lowest  $[\alpha/\text{Fe}]$  ratios because they form later, out of building blocks where  $[\alpha/\text{Fe}]$  has already dropped.

It is worth pointing out that the  $[\alpha/\text{Fe}]$  ratios do not depend on the gas flows (infall and outflow) experienced by the galaxy (Recchi et al. 2008) therefore our results do not depend on specific infall and outflow parameters, which make them particularly robust. However, these parameters affect the overall metallicity of the galaxy, therefore they need to be taken into account in order to check whether our models can correctly reproduce the mass-metallicity relation. As mentioned in the Introduction, Köppen et al. (2007) have already shown that the IGIMF theory is able to reproduce the mass-metallicity relation found by Tremonti et al. (2004) in star-forming galaxies. We are checking, by means of detailed numerical models, that the IGIMF theory is able to reproduce at the same time the mass-metallicity relation and the  $[\alpha/\text{Fe}]$ - $\sigma$  relation in early-type galaxies. This study will be presented in a forthcoming paper.

We have also considered models in which the IMF does not vary with the SFR and, because of the variations of  $\Delta t$  with SFR, these models are compatible with the observations of large elliptical galaxies as well. However, these models produce a  $[\alpha/\text{Fe}]$  vs.  $\sigma$  relation that can be described as a single-slope power-law, whereas the IGIMF models bend down significantly at low masses (and low  $\sigma$ ). This is because the IGIMF becomes particularly steep in the galaxies with the mildest SFRs and this adds to the downsizing effect (namely the decreasing duration of the SFR with increasing mass). From our study therefore, an important conclusion is that a very reliable observable to test the validity of the IGIMF theory is the observation of the  $[\alpha/\text{Fe}]$  ratios in dwarf galaxies. The available data on  $[\alpha/\text{Fe}]$  ratios in low-mass early-type galaxies show indeed some steepening of the  $[\alpha/\text{Fe}]$  vs.  $\sigma$  relation, in agreement with the IGIMF predictions.

We have also tested how much our results depend on the assumption of a variable  $\Delta t$  with stellar mass by computing models with  $\Delta t = 1$  Gyr irrespective of the stellar mass. The agreement between models and observational data is still reasonably good but the curves tend to flatten out too much at large stellar masses compared with the observations (and with the IGIMF models). This indicates that the downsizing remains a fundamental ingredient to understand the chemical properties of early-type galaxies. However, if we check for which  $\Delta t$ -luminous mass relation we obtain the best fit between data and models, it turns out that the downsizing effect must be milder than predicted by THOM05, in the sense that large galaxies form stars for a slightly longer timescale than calculated by THOM05, whereas low-mass galaxies have star formation durations significantly shorter. Although the exact form of the best-fit  $\Delta t$ -luminous mass relation is subject to a number of parameters (IGIMF parameters; parameters regulating the SNIa rate etc.) and might change once larger and more detailed abundance measurements are available, the result of a milder downsizing effect compared to the findings of THOM05 is robust.

Eventually, we have seen that luminosity-weighted  $[\alpha/\text{Fe}]$  ratios agree very well with the mass-weighted ones (with relative differences of a few hundredths of dex at most), in accordance with the results of Matteucci et al. (1998).

We remind the reader that, with our analytical approach to chemical evolution, we are making some important simplifying assumptions. For instance, our computation of the interstellar  $\frac{\alpha}{\text{Fe}}(t)$  given by eq. 15 does not take into account in detail the lifetimes of massive stars. Furthermore, our present calculations do not take into account the variation with time of the metallicity in galaxies, which should also influence the stellar yields. From the various tests performed so far, and from the comparison of our results with numerical results (Thomas et al. 1999; Pipino & Matteucci 2004), we have verified that these assumptions may play only some minor role in determining the zero-point, but not the slope of the predicted  $[\alpha/\text{Fe}]$  vs  $\sigma$  relation. All of these simplifying assumptions will be relaxed in our forthcoming paper, where we will present a numerical approach to the role of the IGIMF in galactic chemical evolution.

The main results of our paper can be summarized as follows:

- Models in which the IGIMF theory is implemented naturally reproduce an increasing trend of  $[\alpha/\text{Fe}]$  with luminous mass (or  $\sigma$ ), as observed in early-type galaxies.
- However, models with constant duration of the star formation produce a  $[\alpha/\text{Fe}]$  vs.  $\sigma$  relation which flattens out too much at large  $\sigma$ . Only models in which the star formation duration inversely correlates with the galactic luminous mass (downsizing) can quantitatively reproduce the observations.
- Models in which the IGIMF is implemented show (at variance with the constant IMF models) a steepening of the  $[\alpha/\text{Fe}]$  vs.  $\sigma$  relation for small galaxies, therefore the IGIMF theory can be tested by observing the  $[\alpha/\text{Fe}]$  in dwarf galaxies. The observations available so far are in agreement with our predictions.
- Luminosity-weighted abundance ratios differ from the mass-weighted ones by a few hundredths of dex at most. This result, already known for constant IMF models, has been confirmed in the IGIMF framework.
- In order to obtain the best fit between our results and the observed  $[\alpha/\text{Fe}]$  ratios in early-type galaxies, the downsizing effect (namely the shorter duration of the star formation in larger galaxies) has to be milder than previously thought.
- The best results are obtained for a cluster mass function  $\xi_{\text{ecl}} \propto M_{\text{ecl}}^{-2.35}$ , indicating that the embedded cluster mass function should have a Salpeter slope.

**Acknowledgements.** We deeply thank Francesca Matteucci for help and support. Discussions with Antonio Pipino are also acknowledged. S.R. acknowledges generous financial support from the FWF through the Lise Meitner grant M1079-N16. F.C. and S.R. acknowledge financial support from PRIN2007 (Italian Ministry of Research) Prot. N. 2007JJC53X. We thank the referee, Daniel Thomas, for very useful comments.

## References

- Abt, H.A., & Levy, S.G. 1976, *ApJS*, 30, 273  
 Anders, E., & Grevesse, N. 1989, *Geochim. Cosmochim. Acta* 53, 197  
 Bower, R.G., Benson, A.J., Malbon, R., et al. 2006, *MNRAS*, 370, 645  
 Burstein, D., Bender, R., Faber, S., & Nolthenius, R. 1997, *AJ*, 114, 1365  
 Calura, F., & Matteucci, F. 2003, *ApJ*, 596, 734  
 Calura, F., & Matteucci, F. 2006, *ApJ*, 652, 889  
 Calura, F., Matteucci, F., & Menci, N. 2004, *MNRAS*, 353, 500  
 Cattaneo, A., Dekel, A., Devriendt, J., Guiderdoni, B., & Blaizot, J. 2006, *MNRAS*, 370, 1651  
 Chabrier, G. 2001, *ApJ*, 554, 1274  
 Chiappini, C., Matteucci, F., & Gratton, R. 1997, *ApJ*, 477, 765  
 Chilingarian, I.V., Cayatte, V., Durret, F., et al. 2008, *A&A*, 486, 85  
 Cimatti, A., Daddi, E., & Renzini, A. 2006, *A&A* 453, 29  
 Cowie, L.L., Songalia, A., Hu, E.M., & Cohen, J.G. 1996, *AJ*, 112, 839  
 Dabringhausen, J., Kroupa, P., & Baumgardt, H. 2009, *MNRAS*, accepted (arXiv:0901.0915)

- De Lucia, G., Springel, V., White, S.D.M., Croton, D., & Kauffmann, G. 2006, *MNRAS*, 366, 499
- Duquennoy, A., & Mayor, M. 1991, *A&A*, 248, 485
- Evans, N.J., Dunham, M.M., Jørgensen, J.K., et al. 2008, *arXiv:0811.1059*
- Gibson, B.K., Loewenstein, M., & Mushotzky, R.F. 1997, *MNRAS*, 290, 623
- Greggio, L. 1997, *MNRAS*, 285, 151
- Greggio, L. 2005, *A&A*, 441, 1055
- Greggio, L., & Renzini, A. 1983, *A&A*, 118, 217
- Hunter, D.A., Elmegreen, B.G., Dupuy, T.J., & Mortonson, M. 2003, *AJ*, 126, 1836
- Jimenez, R., Padoan, P., Matteucci, F., & Heavens, A.F. 1998, *MNRAS*, 299, 123
- Kodama, T., Yamada, T., Akiyama, M., et al. 2004, *MNRAS*, 350, 1005
- Köppen, J., Weidner, C., & Kroupa, P. 2007, *MNRAS*, 375, 673
- Kouwenhoven, M.B.N., Brown, A.G.A., Zinnecker, H., Kaper, L., & Portegies Zwart, S.F. 2005, *A&A*, 430, 137
- Kroupa, P., Tout, C.A., & Gilmore, G. 1993, *MNRAS*, 262, 545
- Kroupa, P., & Weidner, C. 2003, *ApJ*, 598, 1076
- Kuntschner, H., Lucey, J.R., Smith, R.J., Hudson, R.J., & Davies, R.L. 2001, *MNRAS*, 323, 615
- Lada, C.J., & Lada, E.A. 2003, *ARA&A*, 41, 57
- Larsen, S.S., & Richtler, T. 2000, *A&A*, 354, 836
- Larsen, T.I., Sommer-Larsen, J., & Pagel, B.E.J. 2001, *MNRAS*, 323, 555
- Leitherer, C., Schaerer, D., Goldader, J.D., et al. 1999, *ApJS*, 123, 3
- Mannucci, F., Della Valle, M., Panagia, N., et al. 2005, *A&A*, 433, 807
- Maoz, D. 2008, *MNRAS*, 384, 267
- Marigo, P. 2001, *A&A*, 370, 194
- Massey, P. 2003, *ARA&A*, 41, 15
- Massey, P., & Hunter, D.A. 1998, *ApJ*, 493, 180
- Matteucci, F. 1994, *A&A*, 288, 57
- Matteucci, F. 2001, *The Chemical Evolution of the Galaxy*, ASSL, Kluwer Academic Publisher
- Matteucci, F. 2007, *arXiv:0704.0770*
- Matteucci, F., Ponzzone, R., & Gibson, B.K. 1998, *A&A*, 335, 855
- Matteucci, F., & Recchi, S. 2001, *ApJ*, 558, 351
- Nagashima, M., Lacey, C.G., Okamoto, T., et al. 2005, *MNRAS*, 363, L31
- Padovani, P., & Matteucci, F. 1993, *ApJ*, 416, 26
- Pflamm-Altenburg, J., Weidner, C., & Kroupa, P. 2007, *ApJ*, 671, 1550 (PWK07)
- Pilyugin, L.S., & Edmunds, M.G. 1996, *A&A*, 313, 783
- Pipino, A., Kawata, D., Gibson, B.K., & Matteucci, F. 2005, *A&A*, 434, 553
- Pipino, A., & Matteucci, F. 2004, *MNRAS*, 347, 968
- Pipino, A., Silk, J., & Matteucci, F. 2009, *MNRAS*, 392, 475
- Pipino, A., Devriendt, J.E.G., Thomas, D., Silk, J., & Kaviraj, S. 2008, *astro-ph/0810.5753*
- Piskunov, A.E., Belikov, A.N., Kharchenko, N.V., Sagar, R., & Subramaniam, A. 2004, *MNRAS*, 349, 1449
- Recchi, S., Spitoni, E., Matteucci, F., & Lanfranchi, G.A. 2008, *A&A*, 489, 555
- Romano, D., Chiappini, C., Matteucci, F., & Tosi, M. 2005, *A&A*, 430, 491
- Salpeter, E.E. 1955, *ApJ*, 121, 161
- Sansom, A.E., & Northeast, M.S. 2008, *MNRAS*, 387, 331
- Shara, M.M., & Hurley, J.R. 2002, *ApJ*, 571, 830
- Shatsky, N., & Tokovinin, A. 2002, *A&A*, 382, 92
- Siess, L. 2007, *A&A*, 476, 893
- Smith, L.J., & Gallagher, J.S. III 2001, *MNRAS*, 326, 1027
- Thielemann, F.-K., Nomoto, K., & Hashimoto, M. 1993, in *Origin and Evolution of the Elements*, eds. N. Prantzos, E. Vangioni-Flam and M. Cassé, Cambridge Univ. Press, Cambridge, p. 297
- Thomas, D., Greggio, L., & Bender, R. 1999, *MNRAS*, 302, 537
- Thomas, D., Maraston, C., & Bender, R. 2002, *Ap&SS*, 281, 371
- Thomas, D., Maraston, C., Bender, R., & Mendes de Oliveira, C. 2005, *ApJ*, 621, 673 (THOM05)
- Timmes, F.X., Woosley, S.E., & Weaver, T.A. 1995, *ApJS*, 98, 617
- Tremonti, C.A., Heckman, T.M., Kauffmann, G., et al. 2004, *ApJ*, 613, 898
- Tutukov, A.V. 1978, *A&A*, 70, 57
- Tutukov, A.V., & Yungelson, L.R. 1980, in *Close Binary Stars*, eds. M.J. P. Lavee, D.M. Popper and R.K. Ulrich, Reidel, Dordrecht, p. 15
- Valiante, R., Matteucci, F., Recchi, S., & Calura, F. 2009, *NewA*, accepted (*arXiv:0807.2354*)
- van Zee, L., Barton, E.J., & Skillman, E.D. 2004, *AJ*, 128, 2797
- Vázquez, G.A., & Leitherer, C. 2005, *ApJ*, 621, 695
- Weidner, C., & Kroupa, P. 2004, *MNRAS*, 348, 187
- Weidner, C., & Kroupa, P. 2005, *ApJ*, 625, 754
- Weidner, C., & Kroupa, P. 2006, *MNRAS*, 365, 1333
- Weidner, C., Kroupa, P., & Larsen, S.S. 2004, *MNRAS*, 350, 1503
- Weiss, A., Peletier, R.F., & Matteucci, F. 1995, *A&A*, 296, 73
- Whelan, J., & Iben, I.Jr. 1973, *ApJ*, 186, 1007
- Woosley, S.E., & Weaver, T.A. 1995, *ApJS*, 101, 181
- Wyse, R.F.G., Gilmore, G., Houdashelt, M.L., et al. 2002, *New Astron.*, 7, 395
- Zhang, Q., & Fall, S.M. 1999, *ApJ*, 527, L81